

---

# 1

---

## SIGNAL THEORY AND ANALYSIS

---

A *signal*, in general, refers to an electrical waveform whose amplitude varies with time. Signals can be fully described in either the time or frequency domain. This chapter discusses the characteristics of signals and identifies the main tools used for signal processing. Some functions widely used in signal processing are described in Section 1.1. A quick review of the linear system and convolution theory is covered in Section 1.2. Fourier series representation of periodic signals is discussed in Section 1.3. Fourier transform of nonperiodic signals and periodic signals are covered in Sections 1.4 and 1.5, respectively. Section 1.6 describes sampling theory together with signal interpolation. Some advanced sampling and interpolation techniques are reviewed in Section 1.7.

### 1.1 SPECIAL FUNCTIONS USED IN SIGNAL PROCESSING

#### 1.1.1 Delta or Impulse Function $\delta(t)$

The delta function or impulse function  $\delta(t)$  is defined as

$$\begin{aligned}\delta(t) &= \infty && \text{for } t = 0, \\ &= 0 && \text{for } t \neq 0.\end{aligned}$$

and

$$\int_{-\infty}^{\infty} \delta(t) dt = 1. \quad (1.1)$$

## 2 SIGNAL THEORY AND ANALYSIS

On the basis of this definition, one can obtain

$$\int_{-\infty}^{\infty} f(t)\delta(t)dt = f(0)$$

and

$$\int_{-\infty}^{\infty} f(t)\delta(t - t_0)dt = f(t_0).$$

### 1.1.2 Sampling or Interpolation Function $\text{sinc}(t)$

The function  $\text{sinc}(t)$  is defined as

$$\begin{aligned} \text{sinc}(t) &= 1 \quad \text{for } t = 0 \\ &= \frac{\sin(\pi t)}{\pi t} \quad \text{otherwise} \end{aligned}$$

and

$$\int_{-\infty}^{\infty} \text{sinc}(t)dt = 1. \quad (1.2)$$

A  $\text{sinc}(t)$  function for  $t = -4$  to  $4$  is depicted in Fig. 1.1. Notice that  $\text{sinc}(t) = 0$  for all integers of  $t$ , and its local maxima corresponds to its intersection with the  $\cos(\pi t)$ .

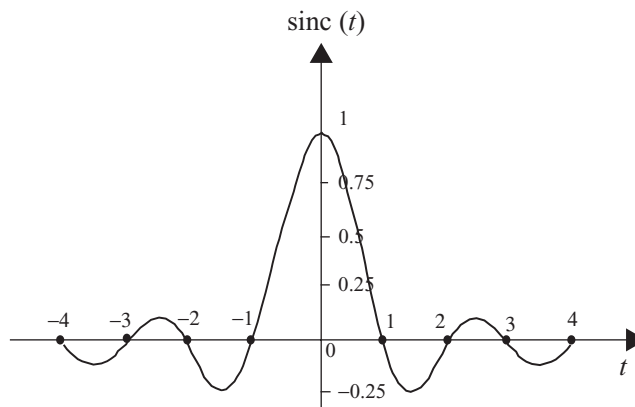


FIGURE 1.1 A  $\text{sinc}(t)$  function.

## 1.2 LINEAR SYSTEM AND CONVOLUTION

A linear system, as shown in Fig. 1.2, can be represented as a box with input  $\underline{x}$ , output  $\underline{y}$  and a system operator  $\mathbf{H}$  that defines the relationship between  $\underline{x}$  and  $\underline{y}$ . Both  $\underline{x}$  and  $\underline{y}$  can be a set of components.

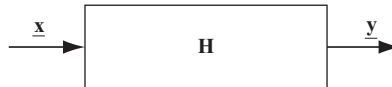


FIGURE 1.2 A linear system.

A system is linear if and only if

$$\mathbf{H}(a\underline{x} + b\underline{y}) = a\mathbf{H}\underline{x} + b\mathbf{H}\underline{y}. \quad (1.3)$$

where  $a$  and  $b$  are constants,  $\underline{x}$  is the system's input signal, and  $\underline{y}$  is the output signal.

In addition, a linear system having the fixed input-output relation

$$\mathbf{H}\underline{x}(t) = \underline{y}(t)$$

is time-invariant if and only if

$$\mathbf{H}\underline{x}(t - \tau) = \underline{y}(t - \tau)$$

for any  $\underline{x}(t)$  and any  $\tau$ . In the following discussion, only the linear and time-invariant system is considered.

Let  $p_\tau(t)$  be a pulse with amplitude  $1/\Delta\tau$  and duration  $\Delta\tau$ ; then any function  $f(t)$  can be represented as

$$f(t) \approx \sum_{n=-\infty}^{\infty} f(n\Delta\tau)p_\tau(t - n\Delta\tau)\Delta\tau. \quad (1.4a)$$

Figure 1.3 illustrates the relationship between  $p_\tau(t)$  and the function  $f(t)$ . Figure 1.3a shows a rectangular polygon with amplitude  $1/\Delta\tau$  and duration  $\Delta\tau$ ; Fig. 1.3b

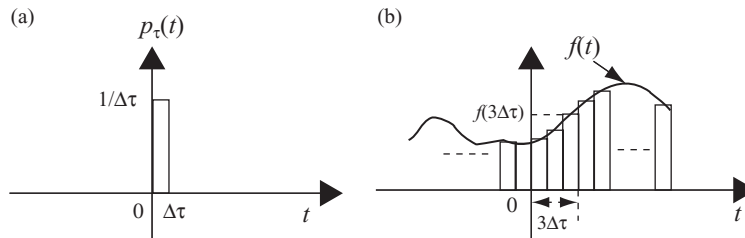


FIGURE 1.3 Graphical representations of a function in terms of pulses.

4 SIGNAL THEORY AND ANALYSIS

displays how a function  $f(t)$  can be approximated by a series of delayed rectangular polygon  $p_\tau(t - n\Delta\tau)$  with amplitude  $f(n\Delta\tau)\Delta\tau$ .

As  $\Delta\tau \rightarrow 0$ ,  $n\Delta\tau \rightarrow \tau$ . Therefore

$$p_\tau(t) \rightarrow \delta(t)$$

and

$$p_\tau(t - n\Delta\tau) \rightarrow \delta(t - \tau).$$

The summation of Eq. (1.4a) then becomes

$$f(t) = \int_{-\infty}^{\infty} f(\tau)\delta(t - \tau)d\tau. \quad (1.4b)$$

Let  $h(t)$  be the impulse response of a system:

$$\mathbf{H} \delta(t) = h(t).$$

Then, for any input function  $x(t)$ , the output function  $y(t)$  can be expressed as

$$\begin{aligned} y(t) &= \mathbf{H} x(t) \\ &= \mathbf{H} \int_{-\infty}^{\infty} x(\tau)\delta(t - \tau)d\tau \\ &= \int_{-\infty}^{\infty} x(\tau)h(t - \tau)d\tau \\ &= x(t) * h(t). \end{aligned} \quad (1.5)$$

where the asterisk (symbol  $*$ ) refers to convolution. If  $x(t) = \delta(t)$ , then

$$\begin{aligned} y(t) &= x(t) * h(t) \\ &= \delta(t) * h(t) \\ &= h(t). \end{aligned}$$

Equation (1.5) states the relationship between the input function  $x(t)$ , the impulse response or system function  $h(t)$ , and the output function  $y(t)$ . It serves as a fundamental equation and is widely used in linear and time-invariant systems. A simple block diagram that illustrates this relationship is shown in Fig. 1.4

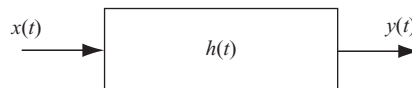


FIGURE 1.4 A time-invariant linear system.

## 1.2.1 Key Properties of Convolution

### 1.2.1.1 Commutative

By letting  $\lambda = t - \tau$ , Eq. (1.5) becomes

$$\begin{aligned}y(t) &= \int_{-\infty}^{\infty} x(\tau)h(t - \tau)d\tau \\ &= \int_{-\infty}^{\infty} x(t - \lambda)h(\lambda)d\lambda \\ &= h(t) * x(t).\end{aligned}$$

Therefore

$$\begin{aligned}y(t) &= x(t) * h(t) \\ &= h(t) * x(t).\end{aligned}\tag{1.6}$$

### 1.2.1.2 Associative

If

$$y(t) = [x(t) * h(t)] * z(t),$$

then

$$\begin{aligned}y(t) &= x(t) * [h(t) * z(t)] \\ &= [x(t) * z(t)] * h(t).\end{aligned}\tag{1.7}$$

### 1.2.1.3 Distributive

If

$$y(t) = x(t) * h(t) + x(t) * z(t),$$

then

$$y(t) = x(t) * [h(t) + z(t)].\tag{1.8}$$

### 1.2.1.4 Timeshift

If

$$y(t) = x(t) * h(t),$$

then

$$\begin{aligned}y(t - \tau) &= x(t - \tau) * h(t) \\ &= x(t) * h(t - \tau).\end{aligned}\tag{1.9}$$

6 SIGNAL THEORY AND ANALYSIS

**1.3 FOURIER SERIES REPRESENTATION OF PERIODIC SIGNALS**

A signal  $g_p(t)$  is called a *periodic signal* with period  $T_0$  if it remains unchanged after it has been shifted forward or backward by  $T_0$ , that is

$$g_p(t) = g_p(t + /- T_0),$$

where  $T_0 = 2\pi/\omega_0$ .

There are three different Fourier series representations for a periodic signal. The first two representations are in terms of trigonometric functions, while the third is in exponential form. The three Fourier series representations of a periodic signal  $g_p(t)$  are described below.

**1.3.1 Trigonometric Fourier Series**

A periodic signal  $g_p(t)$  can be represented as

$$g_p(t) = a_0 + \sum_{n=1}^{\infty} a_n \cos(n\omega_0 t) + \sum_{n=1}^{\infty} b_n \sin(n\omega_0 t), \quad (1.10a)$$

where  $a_n$  and  $b_n$  for  $n = 1, 2, \dots$  can be computed as

$$a_0 = \frac{1}{T_0} \int_0^{T_0} g_p(t) dt, \quad (1.10b)$$

$$a_n = \frac{2}{T_0} \int_0^{T_0} g_p(t) \cos(n\omega_0 t) dt, \quad (1.10c)$$

$$b_n = \frac{2}{T_0} \int_0^{T_0} g_p(t) \sin(n\omega_0 t) dt. \quad (1.10d)$$

**1.3.2 Compact Trigonometric Fourier Series**

Alternatively, a periodic signal  $g_p(t)$  can be represented as

$$g_p(t) = c_0 + \sum_{n=1}^{\infty} c_n \cos(n\omega_0 t + \theta_n), \quad (1.11a)$$

where

$$c_0 = a_0, \quad (1.11b)$$

$$c_n = \sqrt{a_n^2 + b_n^2}, \quad (1.11c)$$

$$\theta_n = \tan^{-1} \frac{b_n}{a_n}. \quad (1.11d)$$

### 1.3.3 Exponential Fourier Series

A periodic signal  $g_p(t)$  can also be represented as

$$g_p(t) = \sum_{n=-\infty}^{\infty} G_n e^{jn\omega_0 t}, \quad (1.12a)$$

where

$$G_n = \frac{1}{T_0} \int_0^{T_0} g_p(t) e^{-jn\omega_0 t} dt,$$

or

$$G_0 = a_0, \quad (1.12b)$$

$$G_n = \frac{a_n - j b_n}{2}, \quad (1.12c)$$

$$G_{-n} = \frac{a_n + j b_n}{2}. \quad (1.12d)$$

**Example 1.1** Figure 1.5 shows a periodic signal  $g_p(t)$ , which is expressed as

$$g_p(t) = \sum_{n=-\infty}^{\infty} g(t - nT_0),$$

with

$$g(t) = A \quad \text{for } -\frac{\tau}{2} \leq t \leq \frac{\tau}{2},$$

$$= 0 \quad \text{otherwise.}$$

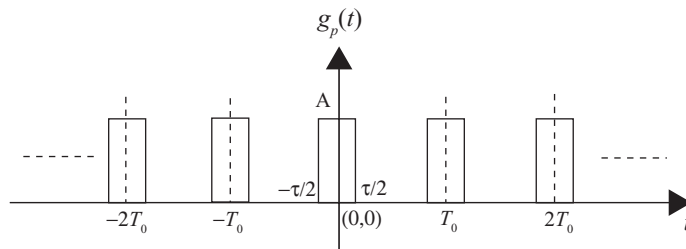


**FIGURE 1.5** A periodic signal  $g_p(t)$ .

8 SIGNAL THEORY AND ANALYSIS

The Fourier series coefficients of  $g_p(t)$  in terms of these three representations can be computed as the following equations show:

1. From Eq. (1.10)

$$\begin{aligned}
 g_p(t) &= a_0 + \sum_{n=1}^{\infty} a_n \cos(n\omega_0 t) + \sum_{n=1}^{\infty} b_n \sin(n\omega_0 t). \\
 a_0 &= \frac{1}{T_0} \int_0^{T_0} g_p(t) dt \\
 &= \frac{1}{T_0} \int_{-\tau/2}^{\tau/2} A dt \\
 &= \frac{A\tau}{T_0}. \\
 a_n &= \frac{2}{T_0} \int_0^{T_0} g_p(t) \cos(n\omega_0 t) dt \\
 &= \frac{2}{T_0} \int_{-\tau/2}^{\tau/2} A \cos n\omega_0 t dt \\
 &= \frac{2A}{n\pi} \sin \frac{n\pi\tau}{T_0}. \\
 b_n &= \frac{2}{T_0} \int_0^{T_0} g_p(t) \sin(n\omega_0 t) dt \\
 &= \frac{2}{T_0} \int_{-\tau/2}^{\tau/2} A \sin(n\omega_0 t) dt \\
 &= 0.
 \end{aligned}$$

2. From Eq. (1.11)

$$\begin{aligned}
 g_p(t) &= c_0 + \sum_{n=1}^{\infty} c_n \cos(n\omega_0 + \theta_n). \\
 c_0 &= a_0 \\
 &= \frac{A\tau}{T_0}. \\
 c_n &= \sqrt{a_n^2 + b_n^2} \\
 &= a_n \\
 &= \frac{2A}{n\pi} \sin \frac{n\pi\tau}{T_0}. \\
 \theta_n &= \tan^{-1} \frac{b_n}{a_n} \\
 &= 0.
 \end{aligned}$$



3. From Eq. (1.12)

$$\begin{aligned}
 g_p(t) &= \sum_{n=-\infty}^{\infty} G_n e^{jn\omega_0 t}. \\
 G_0 &= a_0. \\
 G_n &= G_{-n} \\
 &= \frac{a_n}{2} \\
 &= \frac{A}{n\pi} \sin \frac{n\pi\tau}{T_0} \\
 &= \frac{A\tau}{T_0} \frac{\sin(n\pi\tau/T_0)}{n\pi\tau/T_0} \\
 &= \frac{A\tau}{T_0} \operatorname{sinc}\left(\frac{n\tau}{T_0}\right).
 \end{aligned}$$

Figure 1.6 displays the  $G_n$  for the case when  $A = 1$  and  $\tau = T_0 / 2$ . Notice that the Fourier series coefficients of  $\{G_n\}$  are discrete and the dashed line represents the envelope of  $\{G_n\}$ .

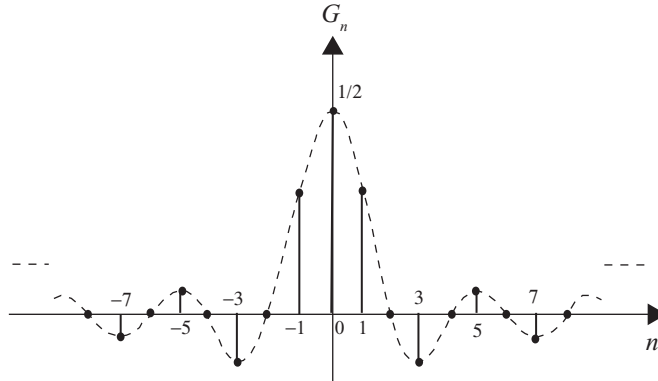


FIGURE 1.6 Fourier series coefficients of a periodic pulse.

**Example 1.2** Let the periodic signal  $g_p(t)$  in Example 1.1 be modified with  $\tau = 0$  and  $A = \infty$ , such that  $A\tau = 1$ :

$$\begin{aligned}
 g_p(t) &= \sum_{n=-\infty}^{\infty} g(t - nT_0) \\
 &= \sum_{n=-\infty}^{\infty} \delta(t - nT_0).
 \end{aligned}$$

10 SIGNAL THEORY AND ANALYSIS

The three Fourier series representations of a periodic impulse train can be computed as follows:

1. From Eq. (1.10)

$$\begin{aligned}
 a_0 &= \frac{1}{T_0} \int_0^{T_0} g_p(t) dt \\
 &= \lim_{\substack{\tau \rightarrow 0 \\ A \rightarrow \infty}} \frac{1}{T_0} \int_{-\tau/2}^{\tau/2} \delta(t) dt \\
 &= \frac{1}{T_0}. \\
 a_n &= \lim_{\substack{\tau \rightarrow 0 \\ A \rightarrow \infty}} \frac{2}{T_0} \int_{-\tau/2}^{\tau/2} \delta(t) \cos(n\omega_0 t) dt \\
 &= \frac{2}{T_0}. \\
 b_n &= 0.
 \end{aligned}$$

Therefore

$$\begin{aligned}
 g_p(t) &= \sum_{n=-\infty}^{\infty} \delta(t - nT_0) \\
 &= \frac{1}{T_0} + \sum_{n=1}^{\infty} \frac{2}{T_0} \cos(n\omega_0 t).
 \end{aligned}$$

2. From Eq. (1.11)

$$\begin{aligned}
 c_0 &= a_0 \\
 &= \frac{1}{T_0}. \\
 c_n &= \sqrt{a_n^2 + b_n^2} \\
 &= a_n \\
 &= \frac{2}{T_0}. \\
 \theta_n &= \tan^{-1} \frac{b_n}{a_n} \\
 &= 0.
 \end{aligned}$$

Therefore

$$\begin{aligned} g_p(t) &= \sum_{n=-\infty}^{\infty} \delta(t - nT_0) \\ &= \frac{1}{T_0} + \sum_{n=1}^{\infty} \frac{2}{T_0} \cos(n\omega_0 t). \end{aligned}$$

3. From Eq. (1.12)

$$\begin{aligned} G_0 &= a_0 \\ &= \frac{1}{T_0}. \\ G_n &= G_{-n} \\ &= \frac{a_n}{2} \\ &= \frac{1}{T_0}. \end{aligned}$$

Therefore

$$\begin{aligned} g_p(t) &= \sum_{n=-\infty}^{\infty} \delta(t - nT_0) \\ &= \sum_{n=-\infty}^{\infty} \frac{1}{T_0} e^{jn\omega_0 t}. \end{aligned}$$

#### 1.4 NONPERIODIC SIGNAL REPRESENTATION BY FOURIER TRANSFORM

A periodic signal  $g_p(t)$  can always be represented in one of the three Fourier series forms described in the previous section. Consider the signal based on exponential representation as shown in Eq. (1.12a), that is

$$g_p(t) = \sum_{n=-\infty}^{\infty} G_n e^{jn\omega_0 t},$$

where  $G_n$  can be derived as

$$G_n = \frac{1}{T_0} \int_0^{T_0} g_p(t) e^{-jn\omega_0 t} dt$$

**12** SIGNAL THEORY AND ANALYSIS

or

$$G_n = \frac{1}{T_0} \int_{-T_0/2}^{T_0/2} g_p(t) e^{-jn\omega_0 t} dt.$$

A nonperiodic signal  $g(t)$  can be considered as a periodic signal  $g_p(t)$  with the period  $T_0 \rightarrow \infty$ :

$$g(t) = \lim_{T_0 \rightarrow \infty} g_p(t).$$

Notice that  $T_0 \rightarrow \infty$  implies  $\omega_0 = (2\pi/T_0) \rightarrow 0$ .

Let  $\omega_0 \approx \Delta\omega$ ; then

$$T_0 G_n = \int_{-T_0/2}^{T_0/2} g_p(t) e^{-jn \Delta\omega t} dt.$$

From the integration shown above, it can be seen that  $T_0 G_n$  is a function of  $n\Delta\omega$ ; therefore, one can define

$$T_0 G_n = G(n\Delta\omega),$$

and

$$\begin{aligned} g_p(t) &= \sum_{n=-\infty}^{\infty} \frac{G(n\Delta\omega)}{T_0} e^{jn \Delta\omega t} \\ &= \sum_{n=-\infty}^{\infty} \frac{G(n\Delta\omega)\Delta\omega}{2\pi} e^{jn \Delta\omega t}. \end{aligned}$$

Now

$$\begin{aligned} g(t) &= \lim_{T_0 \rightarrow \infty} g_p(t) \\ &= \lim_{T_0 \rightarrow \infty} \frac{1}{2\pi} \sum_{n=-\infty}^{\infty} G(n\Delta\omega) e^{jn \Delta\omega t} \Delta\omega \\ &= \frac{1}{2\pi} \int_{-\infty}^{\infty} G(\omega) e^{j\omega t} d\omega. \end{aligned} \tag{1.13}$$

Similarly

$$\begin{aligned} G(\omega) &= \lim_{\Delta\omega \rightarrow 0} G(n\Delta\omega) \\ &= \lim_{T_0 \rightarrow \infty} T_0 G_n \\ &= \int_{-\infty}^{\infty} g(t) e^{-j\omega t} dt. \end{aligned} \tag{1.14}$$

Equations (1.13) and (1.14) are referred to as the *Fourier transform pair*.  $G(\omega)$  in Eq. (1.14) is considered as the direct Fourier transform of  $g(t)$ , while  $g(t)$  in Eq. (1.13) is the inverse Fourier transform of  $G(\omega)$ . The transform pair can also be expressed as

$$G(\omega) = \mathcal{F}[g(t)]$$

and

$$g(t) = \mathcal{F}^{-1}[G(\omega)].$$

The Fourier transform pair can also be expressed symbolically as

$$g(t) \leftrightarrow G(\omega).$$

Some key properties of the Fourier transform are listed below:

1. 
$$G(-\omega) = G^*(\omega) \quad (1.15)$$

where the asterisk (\*) denotes *complex conjugate of*.

2. If  $g(t) \leftrightarrow G(\omega)$ , then

$$G(t) \leftrightarrow 2\pi g(-\omega). \quad (1.16)$$

3. 
$$g(at) \leftrightarrow \frac{1}{|a|} G\left(\frac{\omega}{a}\right). \quad (1.17)$$

4. 
$$g(t - t_0) \leftrightarrow G(\omega)e^{-j\omega t_0}. \quad (1.18)$$

5. 
$$g(t)e^{j\omega_0 t} \leftrightarrow G(\omega - \omega_0). \quad (1.19)$$

6. If  $g_1(t) \leftrightarrow G_1(\omega)$  and  $g_2(t) \leftrightarrow G_2(\omega)$ , then

$$g_1(t) * g_2(t) \leftrightarrow G_1(\omega)G_2(\omega), \quad (1.20)$$

where the asterisk denotes convolution.

7. If  $g_1(t) \leftrightarrow G_1(\omega)$  and  $g_2(t) \leftrightarrow G_2(\omega)$ , then

$$g_1(t)g_2(t) \leftrightarrow \frac{1}{2\pi} G_1(\omega) * G_2(\omega). \quad (1.21)$$

where the asterisk denotes convolution.

14 SIGNAL THEORY AND ANALYSIS

**Example 1.3** Let  $g(t)$  be defined as

$$g(t) = 1 \quad \text{for } -\frac{\tau}{2} \leq t \leq \frac{\tau}{2},$$

$$= 0 \quad \text{otherwise.}$$

The Fourier transform of  $g(t)$  can be computed as

$$G(\omega) = \mathcal{F}[g(t)]$$

$$= \int_{-\infty}^{\infty} g(t)e^{-j\omega t} dt$$

$$= \int_{-\tau/2}^{\tau/2} e^{-j\omega t} dt$$

$$= \tau \frac{\sin \omega\tau/2}{\omega\tau/2}$$

$$= \tau \operatorname{sinc}(\omega\tau/2\pi).$$

Figure 1.7 displays the time domain function  $g(t)$  and its Fourier transform  $G(\omega)$ .

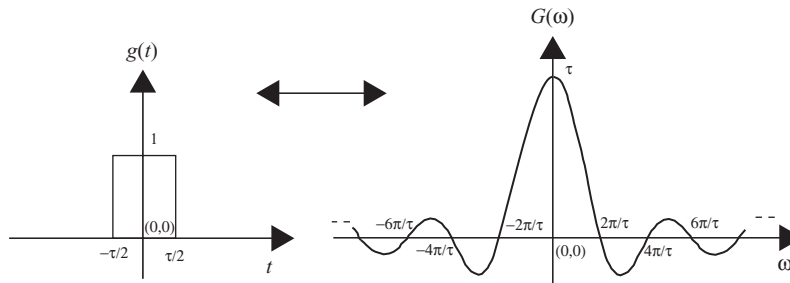


**FIGURE 1.7** A single pulse  $g(t)$  and its Fourier transform  $G(\omega)$ .

By comparing Figs. 1.6 and 1.7, one can see that the Fourier series coefficients of a periodic pulse train is the discrete version of the Fourier transform of a single pulse.

**Example 1.4** Let  $G(\omega)$  be defined as

$$G(\omega) = 1 \quad \text{for } -2\pi f_m \leq \omega \leq 2\pi f_m,$$

$$= 0 \quad \text{otherwise.}$$

The inverse Fourier transform of  $G(\omega)$  can be computed as

$$\begin{aligned}
 g(t) &= \mathcal{F}^{-1}[G(\omega)] \\
 &= \frac{1}{2\pi} \int_{-\infty}^{\infty} G(\omega) e^{j\omega t} d\omega \\
 &= \frac{1}{2\pi} \int_{-2\pi f_m}^{2\pi f_m} e^{j\omega t} d\omega \\
 &= 2f_m \frac{\sin 2\pi f_m t}{2\pi f_m t} \\
 &= 2f_m \operatorname{sinc}(2f_m t).
 \end{aligned}$$

Figure 1.8 displays the frequency domain function  $G(\omega)$  and its inverse Fourier transform  $g(t)$ .

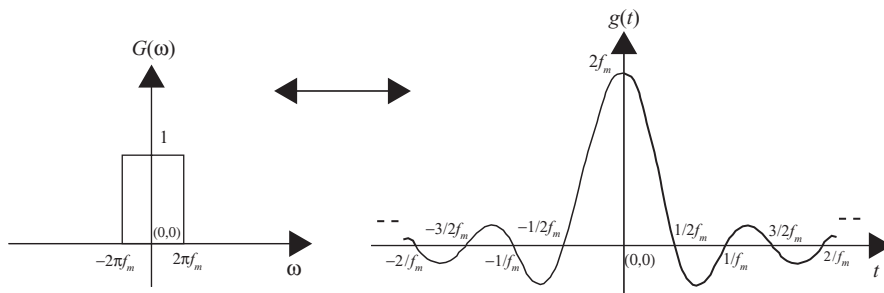


**FIGURE 1.8** A single-pulse frequency spectrum  $G(\omega)$  and its inverse Fourier transform  $g(t)$ .

**Example 1.5** Let  $g(t) = \delta(t)$ , the Fourier transform of  $g(t)$  can be computed as

$$\begin{aligned}
 G(\omega) &= \mathcal{F}[g(t)] \\
 &= \int_{-\infty}^{\infty} g(t) e^{-j\omega t} dt \\
 &= \int_{-\infty}^{\infty} \delta(t) e^{-j\omega t} dt \\
 &= 1.
 \end{aligned}$$

16 SIGNAL THEORY AND ANALYSIS

Therefore,  $\delta(t)$  and 1 are a Fourier transform pair:

$$\delta(t) \leftrightarrow 1.$$

Similarly, if  $G(\omega) = \delta(\omega)$ , then

$$\begin{aligned} g(t) &= \mathcal{F}^{-1}[G(\omega)] \\ &= \frac{1}{2\pi} \int_{-\infty}^{\infty} \delta(\omega) e^{j\omega t} d\omega \\ &= \frac{1}{2\pi}. \end{aligned}$$

Therefore, 1 and  $2\pi \delta(\omega)$  are a Fourier transform pair:

$$1 \leftrightarrow 2\pi \delta(\omega).$$

## 1.5 FOURIER TRANSFORM OF A PERIODIC SIGNAL

Although the Fourier transform was derived from the nonperiodic signal, it can also be used to represent the periodic signal. The Fourier transform of a periodic signal can be computed by first representing the periodic signal in terms of a Fourier series expression, then transforming each Fourier series coefficient (represented in exponential form) into the frequency domain. The following examples illustrate the Fourier transform of periodic signals.

**Example 1.6** Let  $g_p(t)$  be a periodic impulse train, expressed as

$$g_p(t) = \sum_{n=-\infty}^{\infty} \delta(t - nT_0).$$

The Fourier transform of  $g_p(t)$  can be computed by first expressing the periodic signal  $g_p(t)$  in terms of the Fourier series in the exponential form. Thus, from Example 1.2, we obtain

$$\begin{aligned} g_p(t) &= \sum_{n=-\infty}^{\infty} G_n e^{jn\omega_0 t} \\ &= \frac{1}{T_0} \sum_{n=-\infty}^{\infty} e^{jn\omega_0 t}, \end{aligned}$$



where  $\omega_0 = 2\pi/T_0$ . From Example 1.5, the Fourier transform of  $g_p(t)$  can then be computed as

$$\begin{aligned} G(\omega) &= \mathcal{F}[g_p(t)] \\ &= \frac{1}{T_0} \sum_{n=-\infty}^{\infty} \int_{-\infty}^{\infty} e^{-j(\omega - n\omega_0)t} dt \\ &= \frac{2\pi}{T_0} \sum_{n=-\infty}^{\infty} \delta(\omega - n\omega_0). \end{aligned}$$

Figure 1.9 displays the time-domain impulse train  $g_p(t)$  and its Fourier transform  $G(\omega)$ . Both  $g_p(t)$  and  $G(\omega)$  appear to be impulse trains. Notice that the amplitude of the impulse train in the frequency domain is  $\omega_0$  and its spectrum repeated at  $\pm n\omega_0$  with  $n = 1, 2, \dots$  and  $\omega_0 = 2\pi/T_0$ .

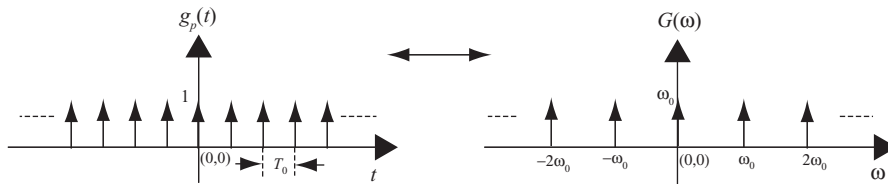


FIGURE 1.9 A periodic impulse train and its Fourier transform.

**Example 1.7** Consider the signal  $g_p(t)$  shown in Example 1.1, expressed as

$$g_p(t) = \sum_{n=-\infty}^{\infty} g(t - nT_0),$$

where

$$\begin{aligned} g(t) &= A \quad \text{for } -\frac{\tau}{2} \leq t \leq \frac{\tau}{2}, \\ &= 0 \quad \text{otherwise.} \end{aligned}$$

The Fourier transform of the periodic pulse train  $g_p(t)$  can be computed in two steps:

*Step 1* A periodic signal should first be expressed in terms of the Fourier series in exponential form:

$$g_p(t) = \sum_{n=-\infty}^{\infty} G_n e^{jn\omega_0 t}.$$

18 SIGNAL THEORY AND ANALYSIS

The Fourier series coefficients  $G_n$  can be computed as

$$\begin{aligned} G_0 &= \frac{A\tau}{T_0}. \\ G_n &= G_{-n} \\ &= \frac{a_n}{2} \\ &= \frac{A}{n\pi} \sin \frac{n\pi\tau}{T_0}. \end{aligned}$$

Therefore,  $g_p(t)$  can be expressed as

$$g_p(t) = \sum_{n=-\infty}^{\infty} \frac{A}{n\pi} \sin \left( \frac{n\pi\tau}{T_0} \right) e^{jn\omega_0 t}.$$

*Step 2* The Fourier transform of  $g_p(t)$  can then be computed as

$$\begin{aligned} G(\omega) &= \mathcal{F}[g_p(t)] \\ &= \int_{-\infty}^{\infty} \sum_{n=-\infty}^{\infty} \frac{A}{n\pi} \sin \left( \frac{n\pi\tau}{T_0} \right) e^{jn\omega_0 t} e^{-j\omega t} dt \\ &= \sum_{n=-\infty}^{\infty} \frac{A}{n\pi} \sin \left( \frac{n\pi\tau}{T_0} \right) \int_{-\infty}^{\infty} e^{-j(\omega - n\omega_0)t} dt. \end{aligned}$$

Example 1.5 has shown that

$$1 \leftrightarrow 2\pi\delta(\omega).$$

Therefore

$$\begin{aligned} G(\omega) &= 2\pi \sum_{n=-\infty}^{\infty} \frac{A}{n\pi} \sin \frac{n\pi\tau}{T_0} \delta(\omega - n\omega_0) \\ &= A \frac{2\pi\tau}{T_0} \sum_{n=-\infty}^{\infty} \frac{\sin(n\pi\tau/T_0)}{n\pi\tau/T_0} \delta(\omega - n\omega_0). \end{aligned}$$

If  $\tau = T_0/2$  and  $A = 1$ , then

$$G(\omega) = \pi \sum_{n=-\infty}^{\infty} \text{sinc}(n/2) \delta(\omega - n\omega_0).$$

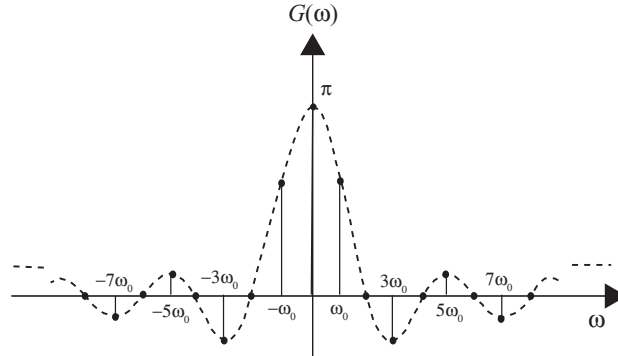


FIGURE 1.10 Fourier transform of a periodic pulse train.

Notice that  $G(\omega)$  is a discrete signal that exists when  $\omega = n\omega_0$  with  $n$  equal to an integer. Figure 1.10 demonstrates the frequency spectrum of  $G(\omega)$  for  $n = -8$  to 8, and its envelope is shown as  $\text{sinc}(n/2)$ .

Note that from Figs. 1.6 and 1.10, for the same periodic sequence  $g_p(t)$ , the amplitude of Fourier series coefficients  $G_n$  and the amplitude of Fourier transform  $G(\omega)$  are the same with a scaling difference of only  $2\pi$ .

## 1.6 SAMPLING THEORY AND INTERPOLATION

The sampling theory states that any signal that is frequency band-limited to  $f_m$  can be reconstructed from samples taken at a uniform time interval of  $T_s \leq 1/(2f_m)$ . The time interval  $T_s = 1/(2f_m)$  is called the *Nyquist interval*, and the corresponding sampling rate is known as the *Nyquist rate*. The sampling theory can be derived as explained below.

Consider a signal  $x(t)$  with its Fourier transform as  $X(\omega)$  and its frequency spectrum band-limited to  $f_m$ . Let  $g_p(t)$  be a unit impulse train as described in Example 1.6. Multiplication of  $x(t)$  with  $g_p(t)$  yields the sampled signal  $x_s(t)$ :

$$\begin{aligned} x_s(t) &= x(t)g_p(t) \\ &= x(t) \sum_{n=-\infty}^{\infty} \delta(t - nT_s). \end{aligned} \quad (1.22)$$

As shown in Example 1.6, a periodic pulse train can be expressed in terms of the Fourier series; that is, with  $\omega_s = 2\pi/T_s$ , are obtains

$$\begin{aligned} x_s(t) &= x(t) \frac{1}{T_s} \sum_{n=-\infty}^{\infty} e^{jn\omega_s t} \\ &= \frac{1}{T_s} \sum_{n=-\infty}^{\infty} x(t) e^{jn\omega_s t}. \end{aligned}$$

20 SIGNAL THEORY AND ANALYSIS

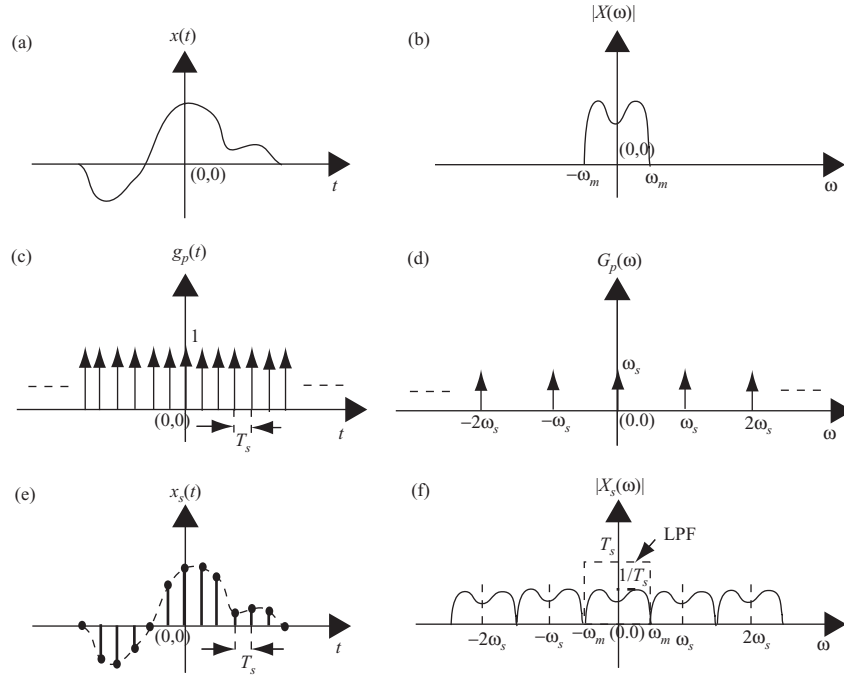


FIGURE 1.11 Graphical representations of the sampling theory.

By taking the Fourier transform of  $x_s(t)$ , one obtains

$$X_s(\omega) = \frac{1}{T_s} \sum_{n=-\infty}^{\infty} X(\omega - n\omega_s). \quad (1.23)$$

This equation states that after multiplication of  $x(t)$  by the unit impulse train  $g_p(t)$ , the new frequency spectra  $X_s(\omega)$  consists of  $X(\omega)$ , plus replica located at  $\omega = \pm n\omega_s$ , for  $n = 0, 1, 2, \dots$ . The amplitude of  $X_s(\omega)$  is attenuated by a factor of  $1/T_s$ .

Figure 1.11 illustrates the sampling theory. The original signal  $x(t)$  and its analog frequency spectrum  $|X(\omega)|$  are shown in Figs. 1.11a and 1.11b. A periodic impulse train  $g_p(t)$  and its spectra are shown in Figs. 1.11c and 1.11d. By multiplying  $x(t)$  with  $g_p(t)$ , one can then display the resultant  $x_s(t)$  in Fig. 1.11e with the corresponding spectra shown in Fig. 1.11f.

From Fig. 1.11f, one can see that to prevent overlap between the neighboring spectra, the sampling frequency  $\omega_s = 2\pi/T_s$  must satisfy the requirement that  $\omega_s \geq (2 \times 2\pi f_m) = 2\omega_m$ .

To reconstruct the original signal  $x(t)$  from the digitized signal  $x_s(t)$ , one needs to filter out the spectrum  $X(\omega)$ , as shown in Fig. 1.11b, from the spectra  $X_s(\omega)$ , as shown in Fig. 1.11f. A lowpass filter (LPF) with a cutoff frequency at  $2\pi f_m$  and a gain equal to  $T_s$  meets the filtering requirement. By passing the  $x_s(t)$  through this lowpass filter, one can reconstruct the original signal  $x(t)$ .

Letting  $H(\omega)$  be such a rectangular LPF, one can compute the time-domain function  $h(t)$  as

$$\begin{aligned} h(t) &= \frac{1}{2\pi} \int_{-2\pi f_m}^{2\pi f_m} T_s e^{j\omega t} d\omega \\ &= 2f_m T_s \frac{\sin(2\pi f_m t)}{2\pi f_m t}. \end{aligned}$$

Let the sampling frequency  $f_s = 2f_m$ ; then

$$h(t) = \text{sinc}(2f_m t). \quad (1.24)$$

In the time domain, passing the signal  $x_s(t)$  through the filter  $h(t)$  is equivalent to having  $x_s(t)$  convolved with  $h(t)$ :

$$\begin{aligned} x(t) &= x_s(t) * h(t) \\ &= \left[ x(t) \sum_{n=-\infty}^{\infty} \delta(t - nT_s) \right] * h(t) \\ &= \sum_{n=-\infty}^{\infty} x(nT_s) \delta(t - nT_s) * \text{sinc}(2f_m t) \\ &= \sum_{n=-\infty}^{\infty} x(nT_s) \text{sinc}(2f_m t - 2f_m nT_s) \\ &= \sum_{n=-\infty}^{\infty} x(nT_s) \text{sinc}(2f_m t - n). \end{aligned} \quad (1.25)$$

Equation (1.25) states that  $x(t)$  can be reconstructed from its discrete samples  $x(nT_s)$  and the interpolation function  $\text{sinc}(2f_m t - n)$ . Notice that  $x(nT_s)$  are all equally spaced with time interval  $T_s$  for integers  $n = -\infty$  to  $\infty$ , and also that  $x(t)$  is a continuous function in the time domain. Thus, Eq. (1.25) can be used to find  $x(t_1)$ , for  $t_1 = nT_s + \Delta T_s$  with  $\Delta < 1$ , based on the discrete values of  $x(nT_s)$ . The new discrete time sequence  $x(t_1)$  can be considered as a resampling of  $x(t)$ , or interpolated from  $x(nT_s)$ .

In practical applications, the resampling process that utilizes the interpolation filter  $\text{sinc}(2f_m t)$  is simplified by two approximations. First, the interpolation filter is chosen with a finite number of sidelobes. For radar image processing, an 8-tap sinc filter is normally used to generate a new interpolated sample. The second approximation involves choosing a finite number of interpolation intervals (or fractional shifts). This means that the value of  $\Delta < 1$  is discrete and finite. A set of 16 sinc filters with a minimum of  $\frac{1}{16}$  interpolation sample intervals, or  $\Delta = \frac{1}{16}$ , serves well for radar

22 SIGNAL THEORY AND ANALYSIS

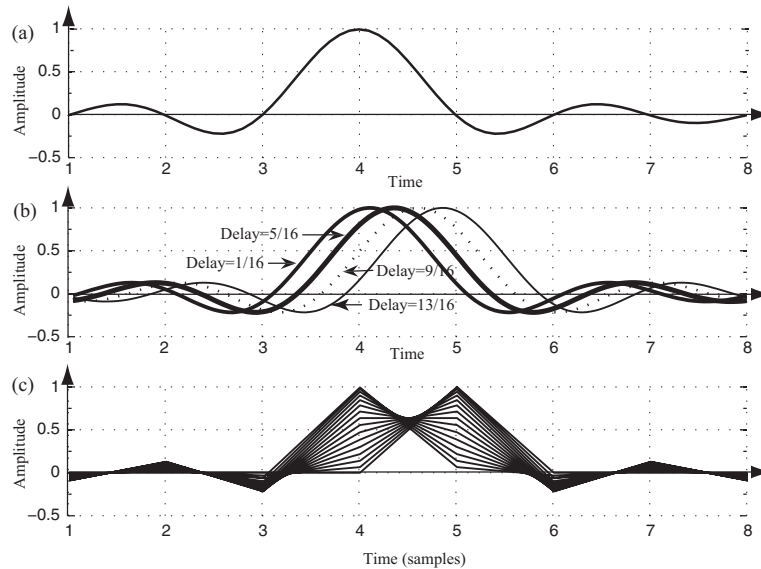


FIGURE 1.12 Interpolation filters.

image processing. This set of 16 sinc filters provides a fractional sample shift from  $\frac{1}{16}, \frac{2}{16}, \dots, \frac{15}{16}$ . The  $\frac{16}{16} = 1$  is not considered a sample shift.

Figure 1.12 displays the waveforms of 16 sets of interpolation filters with each having 8-tap coefficients. Figure 1.12a shows a reference sinc ( $t$ ) function with 5 sidelobes around the mainlobe. The window function is normally applied to the interpolation filter, yet no window or rectangular window is used here for simplification. Figure 1.12b displays four interpolation filters with delays equal to  $\frac{1}{16}, \frac{5}{16}, \frac{9}{16}$ , and  $\frac{13}{16}$  sample intervals with respect to the top reference function, respectively. Figure 1.12c displays the digitized version of all 16 interpolation filters, and each one corresponds to a  $\frac{1}{16}$  sample delay from each other.

Table 1.1 lists the coefficients of the 16 interpolation filters, with each one having 8 coefficients. The first row of filters has a shift of  $\frac{1}{16}$  sample interval, while the last one has  $\frac{16}{16} = 1$  or no sample shift. From Table 1.1 and Fig. 1.12c, one can see that the interpolation filters are symmetric; that is, filter coefficients of row 1 with  $\frac{1}{16}$  sample shift are the same as that of row 15 with  $\frac{15}{16}$  sample shift, except that they are time-reversed. The filter coefficients of rows 1, 5, 9, and 13 of Table 1.1 correspond to the four sinc filters shown in Fig. 1.12b.

To illustrate the principle of resampling based on an interpolation filter, consider a signal  $x(n)$  that consists of three normalized frequencies,  $f_1 = 0.15, f_2 = 0.25$ , and  $f_3 = 0.45$ , and is expressed as

$$x(n) = 0.35 \cos(2\pi n f_1) + 0.2 \sin(2\pi n f_2) - 0.4 \cos(2\pi n f_3),$$

where  $n = 1, 2, \dots, 32$ .

**TABLE 1.1 16 sets of 8-tap interpolation filters**

-0.0203	0.0301	-0.0584	0.9936	0.0662	-0.0321	0.0211	-0.0158
-0.0390	0.0573	-0.1083	0.9745	0.1392	-0.0650	0.0424	-0.0314
-0.0555	0.0808	-0.1489	0.9432	0.2177	-0.0976	0.0629	-0.0464
-0.0693	0.1000	-0.1801	0.9003	0.3001	-0.1286	0.0818	-0.0600
-0.0799	0.1144	-0.2016	0.8469	0.3850	-0.1568	0.0985	-0.0718
-0.0871	0.1238	-0.2139	0.7842	0.4705	-0.1810	0.1120	-0.0811
-0.0908	0.1281	-0.2172	0.7136	0.5550	-0.1998	0.1218	-0.0876
-0.0909	0.1273	-0.2122	0.6366	0.6366	-0.2122	0.1273	-0.0909
-0.0876	0.1218	-0.1998	0.5550	0.7136	-0.2172	0.1281	-0.0908
-0.0811	0.1120	-0.1810	0.4705	0.7842	-0.2139	0.1238	-0.0871
-0.0718	0.0985	-0.1568	0.3850	0.8469	-0.2016	0.1144	-0.0799
-0.0600	0.0818	-0.1286	0.3001	0.9003	-0.1801	0.1000	-0.0693
-0.0464	0.0629	-0.0976	0.2177	0.9432	-0.1489	0.0808	-0.0555
-0.0314	0.0424	-0.0650	0.1392	0.9745	-0.1083	0.0573	-0.0390
-0.0158	0.0211	-0.0321	0.0662	0.9936	-0.0584	0.0301	-0.0203
-0.0000	0.0000	-0.0000	0.0000	1.0000	-0.0000	0.0000	-0.0000

To resample  $x(n)$  to obtain a new set of digitized samples with a 0.5 sample shift, row 8 of the interpolation filter from Table 1.1 is chosen. The new set of data  $x(n + 0.5)$  is computed from Eq. (1.25) by convolving the eight old data samples of  $x(n)$  with the interpolation filter. Figure 1.13 displays the results of the resampling process. Only the effective samples from samples 4–28 of the convolution output are displayed for comparison.

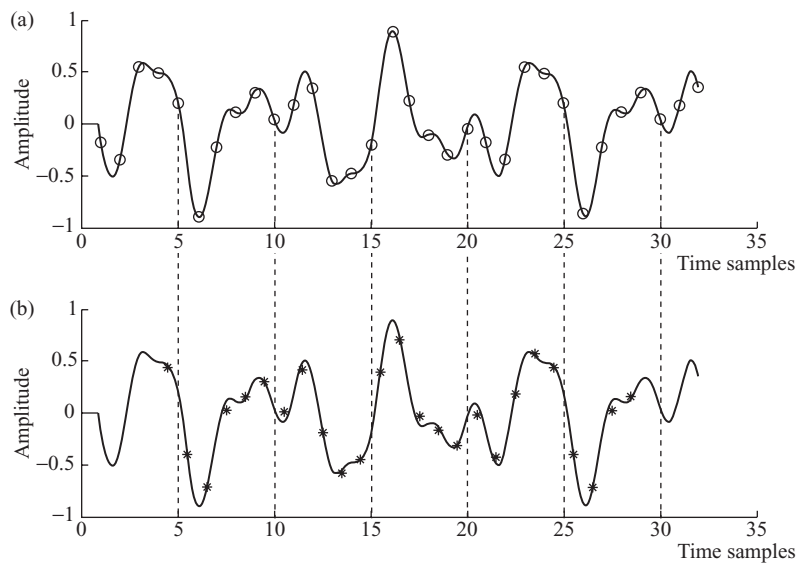


**FIGURE 1.13** Original and half-sample-shifted digital signals.

24 SIGNAL THEORY AND ANALYSIS

Figure 1.13a shows the digitized signal  $x(n)$ , marked by hollow circles ( $\circ$ ), together with the original analog signal  $x(t)$ . Figure 1.13b shows the interpolated (or half-sample-shifted) signal  $x'(n)$ , marked by asterisks (\*), together with the original analog signal  $x(t)$ . As can be seen, the interpolated and digitized signal closely matches the original signal.

The sampling theory discussed so far is based on a unit impulse train. In practice, the impulse train is replaced with a finite-time-duration pulse train. Assuming, that all conditions are the same except that the narrow pulse train with duration  $\tau$  is used, the only difference will be that the amplitude of the Fourier series coefficient  $1/T_s$  is replaced with  $\sin(n\pi\tau/T_s)/n\pi$ . This, in turn, causes Eq. (1.23) to become

$$X_s(\omega) = \sum_{n=-\infty}^{\infty} \frac{\sin(n\pi\tau/T_s)}{n\pi} X(\omega - n\omega_s) \quad (1.26)$$

The lowpass filter defined in Eq. (1.24) can then be applied to the digitized signal  $x_s(t)$ . Accordingly, the  $x(t)$  can again be reconstructed from its digitized samples  $x_s(t)$  by passing the  $x_s(t)$  through a lowpass filter  $h(t)$ . The new reconstruction equation, based on a pulse train with duration  $\tau$ , can be obtained by modifying Eq. (1.25) to become

$$x(t) = \sum_{n=-\infty}^{\infty} \frac{\sin(n\pi\tau/T_s)}{n\pi} x(nT_s) \text{sinc}(2f_m t - n) \quad (1.27)$$

## 1.7 ADVANCED SAMPLING TECHNIQUES

### 1.7.1 Sampling with Bandpass Signal

The sampling theory discussed in Section 1.6 generally applies to baseband signals with a maximum frequency component  $f_m$ . In the case where a signal is band-limited with  $f_l \leq f \leq f_m$  and its center frequency is greater than zero, the Nyquist sampling period  $T_s \leq 1/(2f_m)$  must be modified to reduce the sample rate for signal processing.

Figure 1.14 shows the frequency spectra  $|G(\omega)|$  of a bandpass signal  $g(t)$ . Figure 1.14a shows the frequency spectra  $|G(\omega)|$  of  $g(t)$ , while Fig. 1.14b shows the frequency spectra  $|G_s(\omega)|$  of a sampled signal  $g_s(t)$ . From the sampling theory, the spectrum of the sampled signal will consist of the attenuated spectrum from the original signal and its replica located at  $\pm n\omega_s$ , where  $n = 0, 1, 2, \dots$ . The two-sided spectra,  $a$  and  $b$ , shown in Fig. 1.14a are repeated around  $\pm \omega_s, \pm 2\omega_s \dots$  in Fig. 1.14b. The spectra  $na$  and  $nb$  are the repeated spectra around  $\pm n\omega_s$ .

From Fig. 1.14, it can be seen that no spectrum is overlapped as long as the conditions of  $f_s = 2(f_m - f_l)$  and  $f_l = kf_s$  with  $k$  as an integer are satisfied. If the latter condition is not true, then a higher sampling frequency of  $f_s > 2(f_m - f_l)$  will be needed.



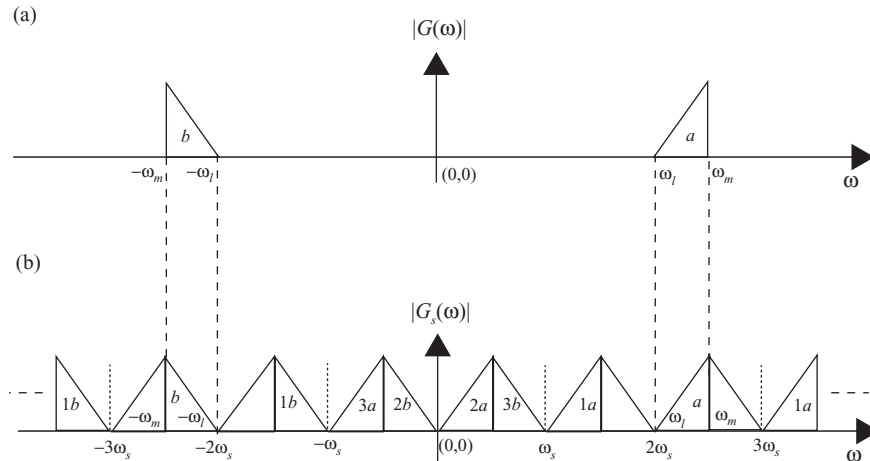


FIGURE 1.14 Frequency spectra of a digitized bandpass signal.

Resampling is necessary for some applications, such as digital communication or audio/video processing. Resampling is used to reduce the computation complexity for signals with a finite bandwidth. Some resampling techniques will now be discussed.

### 1.7.2 Resampling by Evenly Spaced Decimation

Evenly spaced sample decimation can be used to reduce the sample rate by an integral factor. Consider the case of downsampling on a sequence  $x(n)$  by an integer  $M = f_{\text{old}}/f_{\text{new}}$ , where  $f_{\text{old}}$  and  $f_{\text{new}}$  are the old and new sampling rates, respectively. Such a downsampling process can simply retain every  $M$ th sample and discard the others if the frequency aliasing does not occur after downsampling. However, frequency overlap indeed occurs in most downsampling processes. Therefore, a lowpass Finite Impulse Response (FIR) filter is normally used to limit the bandwidth of the signal at a new sampling rate. Both the input sequence  $x(n)$  and the FIR filter function  $h(n)$  operate at an old sample rate  $f_{\text{old}}$ , but the output sequence  $y(m)$  operates at a new sample rate  $f_{\text{new}}$ . Figure 1.15a shows the block diagram of downsampling with a FIR filtering. Figures 1.15b and 1.15c show the signal frequency spectra before and after the decimation for the case when  $M = 2$ . As can be seen from Fig. 1.15c, the signal frequency spectra must be band-limited with  $f_{\text{new}} \geq 2f_m$  to avoid the aliasing problem.

### 1.7.3 Resampling by Evenly Spaced Interpolation

Evenly spaced sample interpolation can be used to increase the sample rate by an integral factor. Consider the case of upsampling on a sequence  $x(n)$  by an integer  $M = f_{\text{new}}/f_{\text{old}}$ , where  $f_{\text{old}}$  and  $f_{\text{new}}$  are the old and new sampling rates, respectively. Upsampling by  $M$  can be implemented by inserting  $M-1$  zeros for every sample of

26 SIGNAL THEORY AND ANALYSIS

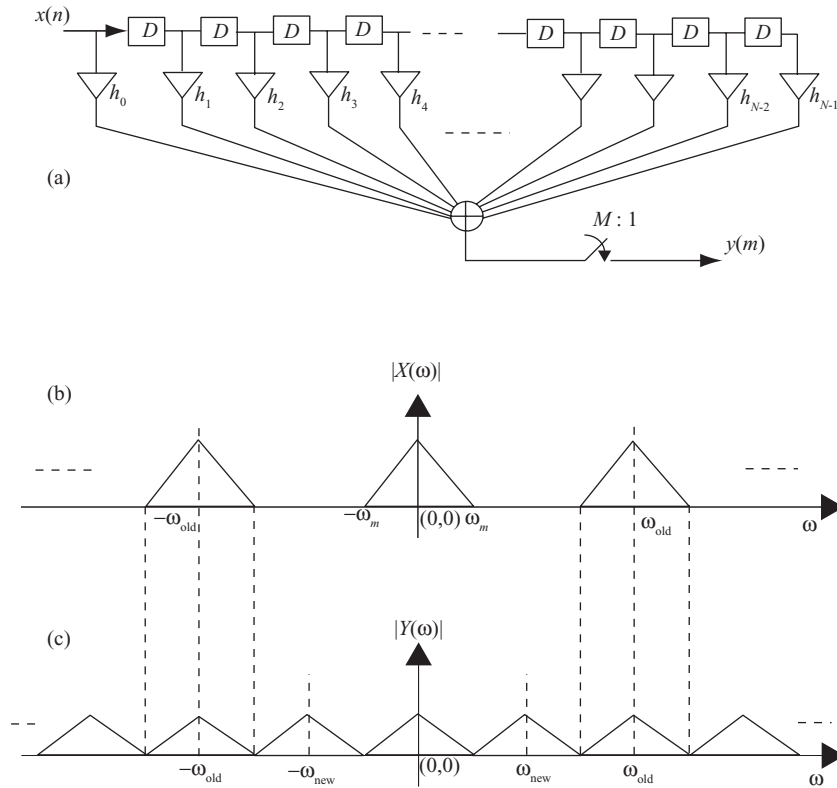


FIGURE 1.15 Downsampling with a FIR filter.

$x(n)$ , and then passing it through a lowpass filter operating at the  $f_{new}$  sampling rate. The lowpass filter is required to filter out the frequency spectra at sampling rate  $f_{new}$ .

Figure 1.16 illustrates the process of interpolation with the sample rate increased by  $M = 3$ . The overall system diagram is shown in Fig. 1.16a, with  $x(n)$  as the input and  $y(m)$  as the output. Figures 1.16b and 1.16c show the original signal  $x(n)$  and its corresponding spectra  $|X(\omega)|$  with sample rate  $f_{old}$ . By inserting two zeros for every sample of  $x(n)$ , one obtains a new signal sequence  $x'(m)$ . Figures 1.16d and 1.16e show the new sequence  $x'(m)$  and its corresponding spectra  $|X'(\omega)|$  with sample rate  $f_{new}$ . After passing  $x'(m)$  through a lowpass filter (LPF), one obtains the interpolated signal  $y(m)$  as shown in Fig. 1.16f, and its frequency spectra are shown in Fig. 1.16g.

### 1.7.4 Resampling by Fractional Rate Interpolation

The interpolation process described in the previous section increases the sample rate with an integral factor. In cases where the sample rate change factor  $M$  is not an

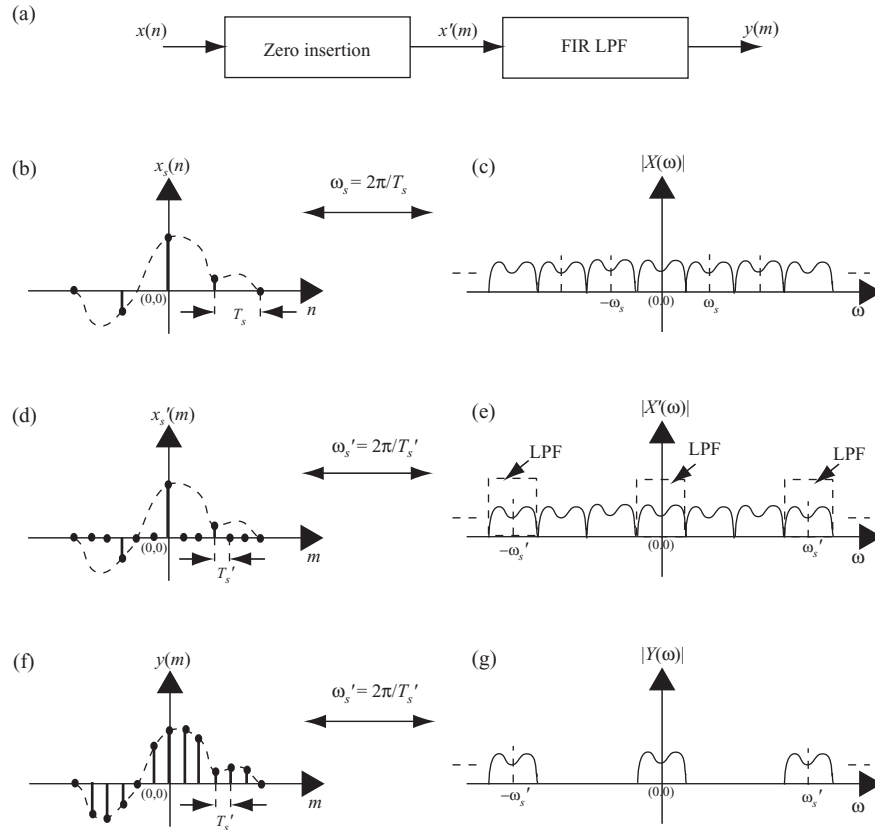


FIGURE 1.16 Interpolation with zero insertion and FIR LPF.

integer, interpolation followed by decimation can be used to obtain any sample rate change. Let the new sample rate change factor be  $M = I + F$ , where  $I$  is an integer and  $F$  is a fractional value. Then  $M = U/D$ , where  $U$  and  $D$  correspond to the upsampling and downsampling rates, respectively.

Consider the case of  $M = 2.5$  with  $U = 5$  and  $D = 2$ . Let the original digitized signal and sampling frequency be  $x(n)$  and  $f_s$ , respectively. To implement the interpolation at a resampling rate of 2.5, one can first upsample  $x(n)$  with sampling frequency equal to  $5f_s$  by inserting four zeros between each sample of  $x(n)$ . The new sequence of samples  $x'(n)$  are then lowpass-filtered (operating at  $5f_s$ ) and followed by downsampling with sampling frequency equal to  $2f_s$ . Figure 1.17a illustrates the overall process of interpolation with  $U = 5$  and  $D = 2$ . Figure 1.17b shows the original signal spectra  $|X(\omega)|$  with sample rate  $f_s$ . By inserting four zeros for every sample of  $x(n)$  followed with a lowpass FIR filter operating at new sampling rate  $f_{\text{new}} = 5f_s$ , one obtains a new sequence  $x'(m)$ . Figure 1.17c shows the spectra of  $|X'(\omega)|$ . The new sequence  $x'(m)$  is then decimated by dumping one out of every sample of  $x'(m)$ .

28 SIGNAL THEORY AND ANALYSIS

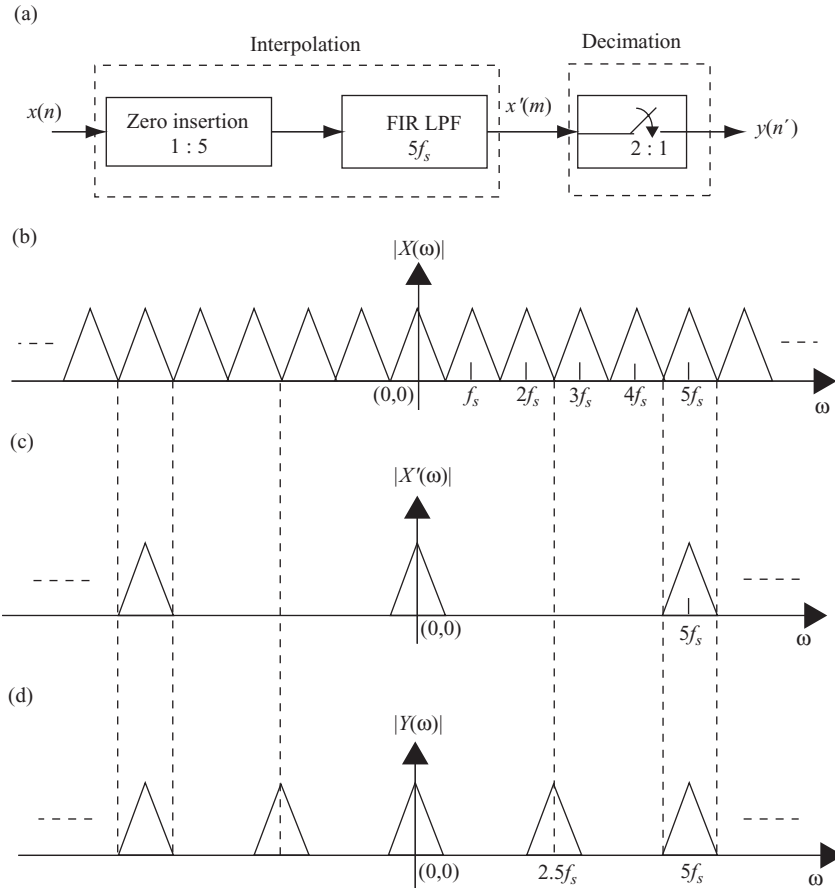


FIGURE 1.17 Fractional rate interpolation with  $M = 2.5$ .

The spectra of interpolated signal  $y(n')$  running at  $2.5f_s$  is shown in Fig. 1.17d. Alternatively, one can just compute one FIR filter output for every two samples shifted into the FIR filter.

### 1.7.5 Resampling from Unevenly Spaced Data

Before discussing the resampling method based on unevenly spaced data, the *Jacobian of transformation* will be explained. This process is used extensively during the transformation between different coordinate systems.

**1.7.5.1 Jacobian of Transformation.** A signal can be transformed from one coordinate system into a different coordinate system. Variables inevitably change during a transformation from one system to another. The transformation can be linear

or nonlinear. The transformation from one system to another may therefore cause an extra factor to appear. This extra factor is called the *Jacobian of transformation*.

Consider the case where  $u = g(v)$ , then  $(du/dv) = (dg(v)/dv) = g'(v)$  and

$$\int_a^b f(u)du = \int_c^d f(g(v))g'(v)dv.$$

The extra factor  $g'(v)$  in this integration is called the *Jacobian of transformation*.

In general, let  $x = g(u,v)$  and  $y = h(u,v)$  be a transformation from  $(x,y)$  domain to  $(u,v)$  domain. Then, the *Jacobian* of transformation, or simply *Jacobian*, is defined as

$$J(u, v) = \frac{\partial(x, y)}{\partial(u, v)} = \begin{vmatrix} \frac{\partial x}{\partial u} & \frac{\partial x}{\partial v} \\ \frac{\partial y}{\partial u} & \frac{\partial y}{\partial v} \end{vmatrix} = \frac{\partial x}{\partial u} \frac{\partial y}{\partial v} - \frac{\partial x}{\partial v} \frac{\partial y}{\partial u}. \quad (1.28)$$

Let  $f(x,y)$  be a function in the  $R(x,y)$  region, and a transformation of  $x = g(u,v)$  and  $y = h(u,v)$  transforms  $f(x,y)$  from  $R(x,y)$  into  $S(u,v)$  region. If  $g(u,v)$  and  $h(u,v)$  have continuous partial derivatives such that the Jacobian is never zero, then

$$\begin{aligned} \iint_R f(x, y) dx dy &= \iint_S f(g(u, v), h(u, v)) \left| \frac{\partial(x, y)}{\partial(u, v)} \right| du dv \\ &= \iint_S f(g(u, v), h(u, v)) J(u, v) du dv. \end{aligned}$$

As an example, let  $x = g(r, \theta) = r \cos \theta$  and  $y = h(r, \theta) = r \sin \theta$ . From Eq. (1.28), the Jacobian of transformation is

$$\begin{aligned} J(r, \theta) &= \frac{\partial x}{\partial r} \frac{\partial y}{\partial \theta} - \frac{\partial x}{\partial \theta} \frac{\partial y}{\partial r} \\ &= \cos \theta \cdot r \cos \theta + r \sin \theta \cdot \sin \theta \\ &= r. \end{aligned}$$

Therefore, the integration shown above becomes

$$\iint_R f(x, y) dx dy = \iint_S f(g(r, \theta), h(r, \theta)) r dr d\theta.$$

This is the well-known rectangular-to-polar coordinate transformation.

The operation of integration in the analog domain is equivalent to summation in the digital domain. The principle of the Jacobian of transformation can therefore be applied to the interpolation or resampling in the digital signal processing field.

30 SIGNAL THEORY AND ANALYSIS

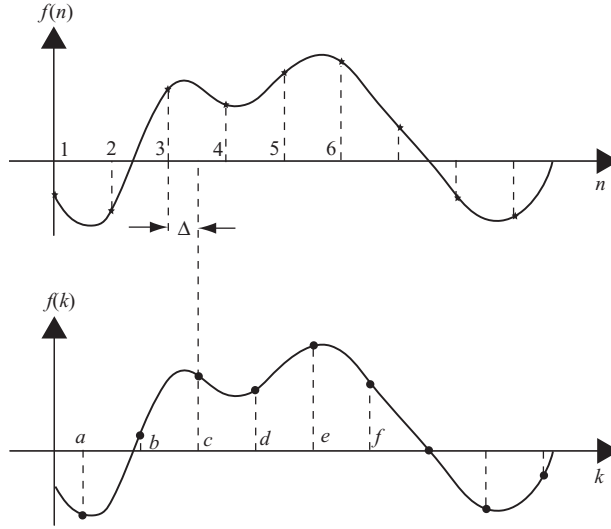


FIGURE 1.18 Interpolation on evenly spaced data.

The sampling theory states that given a set of evenly spaced data  $x(n)$  with sampling frequency  $f_s = 2f_m$ , one can interpolate  $x(n)$  with another set of evenly spaced data  $x(k)$ . Assume that the sampling frequency is normalized to one, that is,  $t = kT_s = k$ . Then Eq. (1.24) becomes

$$x(k) = \sum_{n=-\infty}^{\infty} x(n) \text{sinc}(k - n); \quad k = -\infty \text{ to } \infty. \quad (1.29)$$

The interpolated data  $x(k)$  and the original data  $x(n)$  can be considered as in  $k$  and  $n$  coordinate systems, respectively, and they are related as

$$\begin{aligned} n &= k - \Delta \\ &= g(k), \end{aligned}$$

where  $\Delta$  is a fractional number and  $0 < \Delta < 1$ . The summation of Eq. (1.29) is the discrete convolution of  $x(n)$  with  $\text{sinc}(n)$ , and the data sequence  $x(n)$  is transformed from  $n$  space to  $k$  space. Figure 1.18 shows the interpolation of evenly spaced samples from the view point of transformation between coordinate systems.

The Jacobian of transformation is then

$$J(k) = \frac{dn}{dk} = 1.$$

Therefore, Eq. (1.29) holds without any extra factor for transformation from an evenly spaced system to another evenly spaced system.

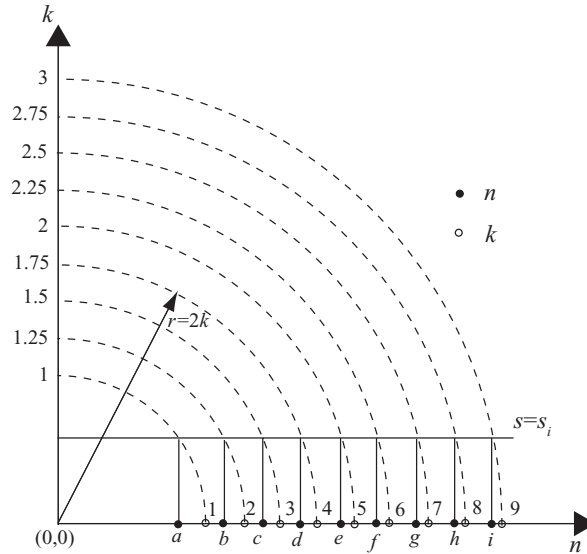


FIGURE 1.19 Generation of unevenly spaced data index.

Now, consider the case where one tries to resample a set of evenly spaced data  $f(k)$  from a set of unevenly spaced data  $f(n)$  with no aliasing. Before the resampling process, the unevenly spaced signal  $f(n)$  must be defined and generated. As an example, the index  $n$  of data  $f(n)$  is generated nonlinearly through the transformation  $g(k)$  as

$$\begin{aligned} n &= g(k) \\ &= \sqrt{(2k)^2 - s^2}, \end{aligned} \quad (1.30)$$

where  $k$  is an evenly spaced variable and equal to half of the radius of a circle with origin at  $(0,0)$ . The symbol  $s$  is a constant and  $s < 2k$ .

Figure 1.19 shows the mapping relation of Eq. (1.30), with the unevenly spaced data index  $n$  obtained from Eq. (1.30) when  $k = 1, 1.25, 1.5, \dots, 3$ , and  $s = s_i < 1$ . The evenly spaced data index  $k$  is the intersection point between the circle with radius  $r = 2k$  and the horizontal axis (abscissa), which is labeled as  $1, 2, 3, \dots$ . The unevenly spaced data index  $n$  is obtained by mapping the intersection point between the circle of radius  $r = 2k$  and the line  $s = s_i$  to the horizontal axis, which is labeled as  $a, b, c, \dots$ .

The Jacobian of transformation from the  $n$  space to  $k$  space is therefore

$$\begin{aligned} J(k) &= \frac{dg(k)}{dk} \\ &= \frac{4k}{\sqrt{4k^2 - s_i^2}} \end{aligned}$$

32 SIGNAL THEORY AND ANALYSIS

This Jacobian is then used to transform the data  $f(n)$  in  $n$  domain to  $f(k)$  in  $k$  domain. The interpolation equation for evenly spaced data shown in Eq. (1.29) therefore becomes

$$\begin{aligned}
 f(k) &= \sum_{n=-\infty}^{\infty} J(k)f(n) \operatorname{sinc}(k - n) \\
 &= \frac{4k}{\sqrt{4k^2 - s_i^2}} \sum_{n=-\infty}^{\infty} f(n) \operatorname{sinc}(k - n); \quad k = -\infty \text{ to } \infty, \quad 2k > s_i.
 \end{aligned}
 \tag{1.31}$$

Notice that in this equation, the variable  $n$  shown in summation serves as an index of the unevenly spaced sample. Figure 1.20 shows, as an example, how the unevenly

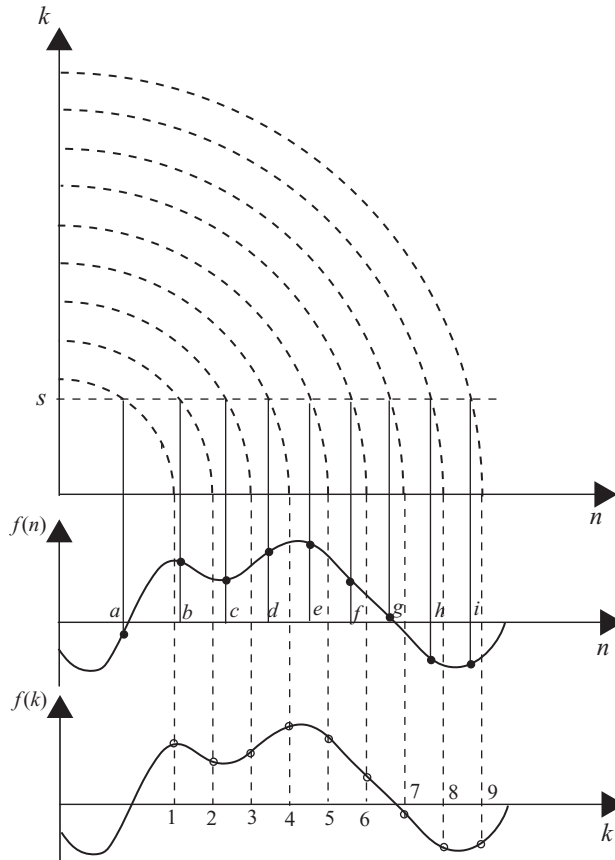


FIGURE 1.20 Relationship between evenly and unevenly spaced data.



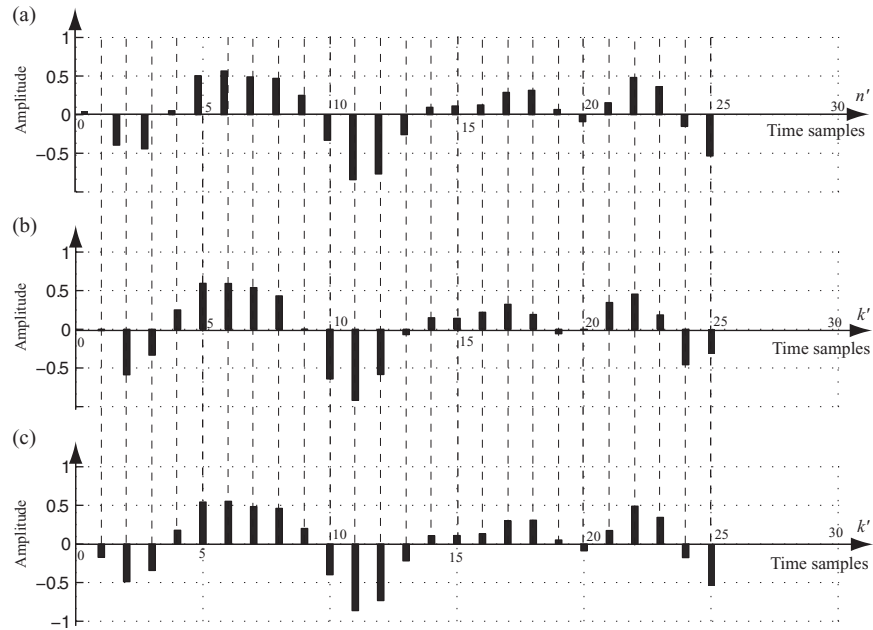


FIGURE 1.21 Interpolation on unevenly spaced data.

spaced data  $f(n)$  and the evenly spaced data  $f(k)$  were transformed from the data indices  $n$  and  $k$ . Given the unevenly spaced data  $f(n)$ , shown as dots ( $\bullet$ ), the interpolated and evenly spaced data  $f(k)$  can therefore be generated from Eq. (1.31), which are denoted by small hollow circles ( $\circ$ ).

The evenly spaced signal  $f(k)$  shown in Fig. 1.13 will now be used to illustrate the interpolation on the basis of the unevenly spaced samples. The signal  $f(k)$  is expressed as

$$f(k) = 0.35 \cos(2\pi k f_1) + 0.2 \sin(2\pi k f_2) - 0.4 \cos(2\pi k f_3),$$

where  $f_1 = 0.25$ ,  $f_2 = 0.45$ , and  $f_3 = 0.15$  are all normalized frequencies. We will reverse the process by generating an unevenly spaced data  $f(n)$  from  $f(k)$  first, then try to interpolate from  $f(n)$  to obtain  $f(k)$ .

The unevenly spaced samples  $f(n)$  are generated by computing the unevenly spaced index  $n$  for various  $k$  from Eq. (1.30). Once the index  $n$  is computed, the value of  $f(n)$  can be obtained.

Consider the case of  $k$  ranging from 0.5 to 6.5 with  $\Delta k = 0.25$  and  $s = 0.75$ ; the corresponding Jacobian can be computed as

$$J(k) = \frac{4k}{\sqrt{4k^2 - (0.75)^2}}.$$

34 SIGNAL THEORY AND ANALYSIS

The 8-tap filters shown in Table 1.1 will be used in this example, and Eq. (1.31) then becomes

$$f(k) = \frac{4k}{\sqrt{4k^2 - (0.75)^2}} \sum_{n=-3}^4 f(n) \operatorname{sinc}(k - n).$$

Figure 1.21a shows the plot of unevenly spaced  $f(n)$  with  $n = \sqrt{4k^2 - (0.75)^2} \approx 2k - \Delta_k$  and  $k = 0.5, 0.75, \dots, 6.5$ ,  $0 < \Delta_k = (0.75)^2/(4k) < 1$ . A total of 25 sinc ( $x$ ) functions are generated, each corresponding to different  $\Delta_k$ . Figure 1.21b displays the interpolated plot of evenly spaced samples  $f(k)$ ,  $k = 0.5, 0.75, \dots, 6.5$ . For comparison purposes, the original evenly spaced signal is displayed in Fig. 1.21c. Notice that Fig. 1.21a is plotted based on the index  $n' = 2n$ , Figs. 1.21b and 1.21c are plotted based on the index  $k' = 4k - 1$ . Notice also that  $f(n)$  appears to be unevenly spaced at the left part of the display, and becomes approximately evenly spaced at the right end of the plot as expected. Just like the original digitized samples shown in Fig. 1.21c, the interpolated signal is evenly spaced and matches quite well with the bottom signal. Only a few samples at both ends differ from the original, because of the edge effect of convolution, which is covered in the next chapter.